

<b>Title</b>	<b>Minimizing the probabilistic magnitude of active vision errors using genetic algorithm</b>
<b>Author(s)</b>	<b>Yang, CCC; Ciarallo, FW</b>
<b>Citation</b>	<b>Computational Cybernetics and Simulation, IEEE International Conference on Systems, Man, and Cybernetics Conference Proceedings, Orlando, Florida, USA, 12-15 October 1997, v. 3, p. 2713-2718</b>
<b>Issued Date</b>	<b>1997</b>
<b>URL</b>	<b><a href="http://hdl.handle.net/10722/45591">http://hdl.handle.net/10722/45591</a></b>
<b>Rights</b>	<b>Creative Commons: Attribution 3.0 Hong Kong License</b>

# Minimizing the Probabilistic Magnitude of Active Vision Errors using Genetic Algorithm

Christopher C Yang<sup>†</sup> and Frank W. Ciarallo<sup>\*</sup>

<sup>†</sup>: Department of Computer Science

The University of Hong Kong

Email: yang@cs.hku.hk

<sup>\*</sup>: Department of Systems and Industrial Engineering

The University of Arizona

## Abstract:

Quantization errors and displacement errors are inevitable in active vision inspection [21,24,25]. In order to obtain high accuracy for dimensioning the entities of three-dimensional CAD models, minimization of these errors is essential. Spatial quantization errors are resulted in digitization. The errors are serious when the size of the pixel is significant compared to the allowable tolerance in the object dimension on the image. In placing the active sensor to perform inspection, displacement of the sensors in orientation and location is common. The difference between observed dimensions obtained by the displaced sensor and the actual dimensions is defined as *displacement errors*. The density functions of quantization errors and displacement errors depend on camera resolution and camera locations and orientations. We use genetic algorithm to minimize the probabilistic magnitude of the errors subject to the sensor constraints, such as the resolution, field-of-view, focus, and visibility constraints. Since the objective functions and the constraint functions are both complicated and nonlinear, traditional nonlinear programming may not be efficient and trapping at a local minimum may occur. Using crossover operations, mutation operations, and the stochastic selection in genetic algorithm, trapping can be avoided.

## 1. Introduction

Errors are inherent in active vision, and they affect the accuracy of inspection. For example, the potential errors are quantization errors, displacement errors, illumination errors, parallax, and sensor motions. Illumination errors, parallax, and sensor motions can be minimized to a negligible level by

careful design and control of the environment. However, quantization errors and displacement errors are inevitable. Kamgar-Parsi [11], Blostein [1], and Ho [10] have investigated spatial quantization errors. Griffin [9] discussed an approach to integrate the errors inherent in the visual inspection to determine the sensor capability for inspecting a specified part dimension using binary images. Su et al. [16], Renders et al. [14], Menq et al. [12], Chen et al. [3], Veitschegger et al. [20], Bryson [2], and Smith et al. [15] have studied the positional and orientational errors of robot manipulators. Yang et al. [4,22,23,26] have examined both the quantization errors and displacement errors in active vision inspection and derived the density functions of the total error.

The sensor settings are constrained by the sensor constraints, such as resolution constraints, focus constraints, field-of-view constraints, and visibility constraints. All of the sensor settings that are to be used of as part of an inspection plan must satisfy this constraint. Cowan and Kovesi [5,6,7], Tarabanis et al. [17,18,19], and Yang and Marefat [25] have examined these constraints and proposed algorithms to obtain potential sensor settings.

Given the density functions of the active vision errors and the formulation of the sensor constraints, it is desired to minimize the active vision errors (maximize inspection accuracy) subject to the sensor constraints. In this paper, we propose to use the genetic algorithm to perform the optimization. Genetic algorithms have shown excellent performance in optimization with complicated and non-linear objective and constraint functions. Compared to traditional non-linear programming [8], it is more efficient and avoids trapping at a local minimum.

## 2. Active Vision Errors

Without careful control, quantization errors and displacement errors can produce significant measurement errors in active vision inspection. For example, a sensor placed very close to an inspected edge segment has high resolution on the image plane, however, the displacement errors from this setting may be too large.

### 2.1 Quantization Errors

Spatial quantization errors affect the accuracy of inspection seriously when the size of the pixel is significant compared to the allowable tolerance in object dimension on the image. In digitization, a quantized sample indicates itself as part of the object image if and only if the edge segment covers more than half of the pixel. Using traditional edge detection, a point in the image can only be located up to one pixel of accuracy. Figure 1 shows a line segment on a two-dimensional array of pixels.

The density functions of the horizontal and vertical quantization errors are derived as [22,23,26]:

For x-direction:

$$f_{\epsilon_{qx}}(\epsilon_{qx}) = \begin{cases} -\frac{1}{r_x^2} \epsilon_{qx} + \frac{1}{r_x} & 0 \leq \epsilon_{qx} \leq r_x \\ \frac{1}{r_x^2} \epsilon_{qx} + \frac{1}{r_x} & -r_x \leq \epsilon_{qx} \leq 0 \\ 0 & \text{else} \end{cases}$$

where  $r_x$  is the horizontal pixel size.

For y-direction:

$$f_{\epsilon_{qy}}(\epsilon_{qy}) = \begin{cases} -\frac{1}{r_y^2} \epsilon_{qy} + \frac{1}{r_y} & 0 \leq \epsilon_{qy} \leq r_y \\ \frac{1}{r_y^2} \epsilon_{qy} + \frac{1}{r_y} & -r_y \leq \epsilon_{qy} \leq 0 \\ 0 & \text{else} \end{cases}$$

where  $r_y$  is the vertical pixel size

Using a geometric approximation, the two-dimensional quantization errors' density functions,  $f_{\epsilon_q}(\epsilon_q)$ , is:

$$f_{\epsilon_q}(\epsilon_q) = \frac{1}{|\cos \gamma|} \int_{-\infty}^{\infty} f_{\epsilon_{qx}} \left( \tan \gamma \left( \frac{1}{\sin \gamma} \tilde{\epsilon}_q - \tau \right) \right) f_{\epsilon_{qy}}(\tau) d\tau$$

where  $\gamma$  is the angle between the line segment and the horizontal axis of the image plane.

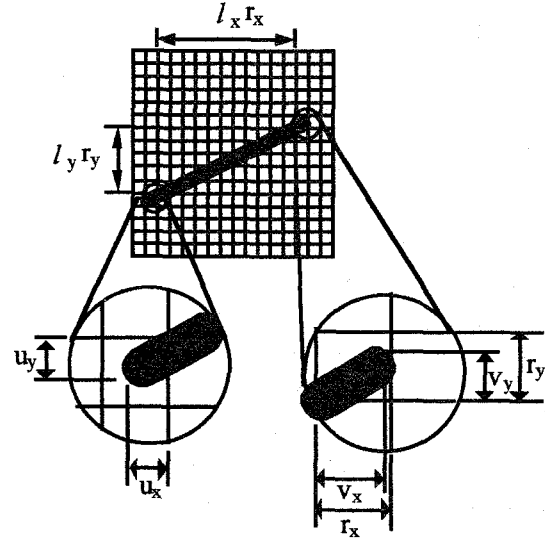


Figure 1 A line on a two-dimensional array of pixels. The horizontal resolution is  $r_x$  and the vertical resolution is  $r_y$ .

### 2.2 Displacement Errors

In active vision inspection, we place the sensors by the active head; there are usually errors in the final position and orientation. If the sensor location and orientation are different from the planned sensor setting (i.e. there is sensor displacement), the same edge segments may be observable, but the dimension measured will be inaccurate. The difference between the observed dimensions and the actual dimensions is defined as *displacement errors*. Figure 2 gives an illustration of the displacement errors.

The displacement errors are derived based on the perspective transformation. The details of derivation can be found in [4,22,26]. The density functions of the horizontal and vertical displacement errors of a point  $(u,v)$  on the image are:

For x-direction:

$$f_{\varepsilon_{dx}}(\varepsilon_{dx}) = \frac{\sigma_{\xi}\sigma_{\chi}\sqrt{1-r_{\xi\chi}^2}}{\pi g_1(\varepsilon_{dx})} \exp\left(-\frac{\mu_{\chi}^2}{2 g_1(\varepsilon_{dx})}\left(\varepsilon_{dx}^2 + \frac{g_2(\varepsilon_{dx})^2}{\sigma_{\chi}^2}\right)\right) + \frac{g_2(\varepsilon_{dx}) \mu_{\chi}\sigma_{\xi}}{\sqrt{2\pi} g_1(\varepsilon_{dx})^{3/2}} \exp\left(-\frac{\mu_{\chi}^2 \varepsilon_{dx}^2}{2 g_1(\varepsilon_{dx})}\right) \operatorname{erf}\left(\frac{g_2(\varepsilon_{dx}) \mu_{\chi}}{\sigma_{\chi}\sqrt{2(1-r_{\xi\chi}^2)g_1(\varepsilon_{dx})}}\right)$$

For y-direction:

$$f_{\varepsilon_{dy}}(\varepsilon_{dy}) = \frac{\sigma_{\xi}\sigma_{\chi}\sqrt{1-r_{\xi\chi}^2}}{\pi h_1(\varepsilon_{dy})} \exp\left(-\frac{\mu_{\chi}^2}{2 h_1(\varepsilon_{dy})}\left(\varepsilon_{dy}^2 + \frac{h_2(\varepsilon_{dy})^2}{\sigma_{\chi}^2}\right)\right) + \frac{h_2(\varepsilon_{dy}) \mu_{\chi}\sigma_{\xi}}{\sqrt{2\pi} h_1(\varepsilon_{dy})^{3/2}} \exp\left(-\frac{\mu_{\chi}^2 \varepsilon_{dy}^2}{2 h_1(\varepsilon_{dy})}\right) \operatorname{erf}\left(\frac{h_2(\varepsilon_{dy}) \mu_{\chi}}{\sigma_{\chi}\sqrt{2(1-r_{\xi\chi}^2)h_1(\varepsilon_{dy})}}\right)$$

where  $g_1(\varepsilon_{dx}) = \sigma_{\xi}^2 - 2r_{\xi\chi}\sigma_{\xi}\sigma_{\chi}\varepsilon_{dx} + \sigma_{\chi}^2\varepsilon_{dx}^2$ ,  
 $g_2(\varepsilon_{dx}) = \sigma_{\xi} - r_{\xi\chi}\sigma_{\chi}\varepsilon_{dx}$ ,  
 $h_1(\varepsilon_{dy}) = \sigma_{\xi}^2 - 2r_{\xi\chi}\sigma_{\xi}\sigma_{\chi}\varepsilon_{dy} + \sigma_{\chi}^2\varepsilon_{dy}^2$ ,  
 $h_2(\varepsilon_{dy}) = \sigma_{\xi} - r_{\xi\chi}\sigma_{\chi}\varepsilon_{dy}$ ,  
 $\zeta$  and  $\xi$  are the numerators of the horizontal and vertical displacement errors,  
 $\chi$  is the denominator of the horizontal and vertical displacement errors.

The density functions of horizontal and vertical displacement errors for a line segment are then derived as:

For x-direction:

$$f_{\varepsilon_{dx}}(\varepsilon_{dx}) = \int_{-\infty}^{\infty} f_{\varepsilon_{dx_1}}(\varepsilon_{dx} + \tau) f_{\varepsilon_{dx_2}}(\tau) d\tau$$

For y-direction:

$$f_{\varepsilon_{dy}}(\varepsilon_{dy}) = \int_{-\infty}^{\infty} f_{\varepsilon_{dy_1}}(\varepsilon_{dy} + \tau) f_{\varepsilon_{dy_2}}(\tau) d\tau$$

The density functions of two-dimensional displacement errors are derived similar to the quantization errors using a geometric approximation:

$$\tilde{f}_{\varepsilon_d}(\tilde{\varepsilon}_d) = \frac{1}{|\cos \gamma|} \int_{-\infty}^{\infty} f_{\varepsilon_{dx}}\left(\tan \gamma \left(\frac{1}{\sin \gamma} \tilde{\varepsilon}_d - \tau\right)\right) f_{\varepsilon_{dy}}(\tau) d\tau$$

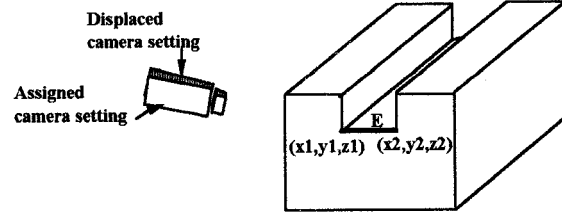


**Figure 2** An edge segment, E, which is the width of the slot on the component, with end points, (x1,y1,z1) and (x2,y2,z2), is dimensioned by the camera with the assigned setting as shown. However, due to displacement errors, the displaced camera setting could undesirably affect the measurement.

### 2.3 Integrating Quantization and Displacement Errors

Given the density functions of the quantization errors and displacement errors, we integrate both to obtain the total error in dimensional inspection using active vision. The total inspection error,  $\varepsilon_i$ , is the sum of the quantization errors and the displacement errors. Its density function is:

$$f_{\varepsilon_i}(\varepsilon_i) = \int_{-\infty}^{\infty} f_{\varepsilon_q}(\varepsilon_i - \tau) f_{\varepsilon_d}(\tau) d\tau$$

### 3. Sensor Constraints

Visual inspection has become popular because of the advance of computer and imaging technologies, however, we need careful sensor placement to make sure all the sensor constraints are satisfied. In this section, we discuss resolution constraints, focus constraints, field-of-view constraints, and visibility constraints.

#### 3.1 Resolution Constraints

In order to obtain a desired accuracy in measured dimensions of a line segment on the image, a minimum resolution is needed. A minimum resolution of the line segment on image requires a maximum distance between the corresponding edge segment of the object and the sensor. We can compute the maximum distance in terms of the focal length, and the distance between the image plane and

the lens. Using this formulation, we can obtain a locus of points (a viewing sphere) that give the maximum bound of the viewing locations.

### 3.2 Focus Constraints

In order to keep the image in focus, we need a lower bound and an upper bound for the distance between the sensor and the inspected edge segment. For any lens settings of the sensors, there is a *focus distance*, at which a point is perfectly focused on the image plane. Other points within a range of the focus distance are in focus, if the diameter of the blur circle of each point is less than the minimum pixel dimension. Based on the focus distance, we can find the maximum and minimum distance such that any points within these distances are in focus. The difference between the maximum and minimum distance is the *depth of field*.

### 3.3 Field-of-View Constraints

The sensor's field-of-view provides a minimum distance between the sensor and the inspected edge segment. A circular cone, *field-of-view cone*, is constructed to compute the minimum distance between the sensor and the edge segment. The vertex angle,  $\alpha$ , of the field-of-view cone depends on the minimum dimension of the image plane, and the distance between the image plane and the lens center.

### 3.4 Visibility Constraints

Cowan and Kovesi, and Tarabani et al. have used the structure of an object and the entities to be observed to construct a region such that all entities are visible. However, this methodology is not as efficient as the aspect graph methodology [27]. An aspect graph is a graph representation of all the characteristic views of an object. Each node of the graph corresponds to a distinct characteristic view of an object. Given a set of entities, we can obtain all the viewing domains that are capable of observing these entities. If a different set of entities is to be inspected, the corresponding set of viewing domains can be found based on the aspect graph without reconstructing all of the viewing domain boundaries [21].

## 4. Optimization by Genetic Algorithm

In order to obtain inspections with high accuracy, we determine the optimized sensor settings

such that the active vision errors are minimized and the sensor constraints are satisfied. The objective of the optimization is to maximize the accuracy of inspection. In other words, we minimize the probability that the errors are outside an acceptable tolerance. The constraints of the optimization are the sensor constraints as described in Section 3.

In this work, we utilize a genetic algorithm to perform the optimization. In our experience, when using traditional non-linear programming, such as gradient search, penalty approach etc., trapping at local minimum occurs occasionally. Moreover, its performance is not consistent. On the other hand, genetic algorithm performs more consistently. Because of the random generation process (mutation operation) in genetic algorithm, trapping at a local minimum does not occur.

### 4.1 Genetic Algorithm

#### Initialization of Population

A chromosome represents a sensor setting. The genes in a chromosome represent the locations and orientations of sensor settings, which are binary numbers. A chromosome has six sets of genes, three of them correspond to the three parameters of locations, and the other three of them correspond to the three parameters of orientations. The higher number of genes ( $M$ ) in a chromosome, the higher precision the parameters of translations and orientations are. Initially,  $N$  numbers of chromosomes are generated randomly. For each chromosome,  $C_i$ , we compute the probability ( $P_i$ ) that the active vision errors are over the given tolerance. ( $i = 1, 2, \dots, N$ )

#### Reproduction

Reproduction is the selection of a new population. A chromosome that has lower  $P_i$  has a better chance of being selected. Each chromosome occupies a certain number of slots on a roulette wheel inversely proportional to its  $P_i$ . Spinning the roulette wheel  $N$  times, we select  $N$  chromosomes for the new population. According to the genetic inheritance, the best chromosomes get more copies, the average stays even, and the worst die off.

### Crossover and Mutation

There are two recombination operations, crossover and mutation. The crossover operates between a pair of chromosome and the mutation operates on a single chromosome.

**Crossover:** The probability of crossover,  $P_c$ , gives us the expected number  $P_c N$  of chromosomes that should undergo the crossover operation. For each chromosome, we generate a random number,  $X$ , between 0 and 1. If  $X$  is less than  $P_c$ , the chromosome is selected for crossover. For each pair of selected chromosomes, we generate a random number,  $Y$ , between 0 and  $M-1$ .  $Y$  indicates the position of the crossing point. The coupled chromosomes exchange genes at the crossover point. If the crossover chromosome does not satisfy the sensor constraints, it does not survive (it is eliminated).

**Mutation:** Mutation is performed on a bit-by-bit basis. The probability of mutation,  $P_m$ , gives us the expected number of mutated bits  $P_m M N$ . Every bit in all chromosomes of the whole population has an equal chance to undergo mutation. For each chromosome and for each bit within the chromosome, we generate a random number,  $Z$ , between 0 and 1. If  $Z$  is less than  $P_m$ , we mutate the bit. Similar to the crossover operation, if the mutated chromosome does not satisfy the sensor constraints, it does not survive (it is eliminated).

### Convergence

After reproduction, crossover, and mutation, the new population is ready for the next generation. The evolution of the solution continues until in this way, repeating these step until the system converges. This occurs when the total of  $P_i$  for the whole population decreases less than a small value,  $\delta$ , for a few generations.

### 5. Conclusion

In this paper, we determine the optimized sensor settings for dimensioning a set of edge segments based on the active vision errors and the sensor constraints. We consider the quantization errors and displacement errors in active vision inspections. The density functions of these errors are used as objective functions in the optimizations. The resolution

constraints, focus constraints, field-of-view constraints, and visibility constraints are used as the constraint functions. We use the genetic algorithm for optimization, which does not have the problem of trapping at local minimum as the traditional non-linear programming.

### References

- [1] Blostein, S. D., and Huang, T. S., "Error Analysis in Stereo Determination of 3-D Point Positions," *IEEE Transactions on Pattern Analysis and Machine Intelligence*, Vol. 9, No. 6, November, 1987.
- [2] Bryson, S., "Measurement and Calibration of Static Distortion of Position Data from 3D Trackers," *SPIE Vol. 1669 Stereoscopic Displays and Applications III*, 1992.
- [3] Chen, J., and Chao, L. M., "Positioning Error Analysis for Robot Manipulators with All Rotary Joints," *IEEE International Conference on Robotics and Automation*, San Francisco, CA, April, 1986.
- [4] Ciarallo, F. W., Yang, C. C., and Marefat, M. M., "Displacement Errors in Active Visual Inspection," *Proceedings of IEEE International Conference on Robotics and Automation*, Minneapolis, Minnesota, April 22-28, 1996.
- [5] Cowan, C. K., and Kovesi, P. D., "Automatic Sensor Placement for Vision Task Requirements," *IEEE Transactions on Pattern Analysis and Machine Intelligence*, vol.10, no.3, 1988.
- [6] Cowan, C. K., and Kovesi, P. D., "Determining the Camera and Light Source Location for A visual Task", *IEEE International Conference on Robotics and Automation*, 1988.
- [7] Cowan, C. K., "Automatic Camera and Light Source Placement Using CAD Models," *IEEE Workshop on Direction in Automated CAD-Based Vision*, 1991.
- [8] Crosby, K., Yang, C. C., Marefat, M. M., Ciarallo, F. W., "Camera Settings for Dimensional Inspection Using Displacement and Quantization Errors" *IEEE International Conference on Robotics and Automation*, Albuquerque, NM, April, 1997.
- [9] Griffin, P. M. and Villalobos, J. R. "Process Capability of Automated Visual Inspection System," *IEEE Transactions on Systems, Man, and Cybernetics*, Vol. 22, No. 3, 1992.
- [10] Ho, C. S., "Precision of Digital Vision Systems," *IEEE Transactions on Pattern Analysis and Machine Intelligence*, Vol. 5, No. 6, Nov, 1983.
- [11] Kamgar-Parsi, B., and Kamgar-Parsi, B., "Evaluation of Quantization Error in Computer

- Vision," *IEEE Transactions on Pattern Analysis and Machine Intelligence*, Vol. 11, No. 9, September, 1989.
- [12] Menq, C. H., and Borm, J. H., "Statistical Measure and Characterization of Robot Errors," *Proceedings of IEEE International Conference on Robotics and Automation*, 1988.
- [13] Paul, R. P., Chapter 4 *Differential Relationships, Robot Manipulators: Mathematics, Pro-gramming, and Control*, The MIT Press, Cambridge, Massachusetts and London, England.
- [14] Renders, J. M., Rossignol, E., Becquet, M., and Hanus, R., "Kinematic Calibration and Geometrical Parameter Identification for Robots," *IEEE Transactions on Robotics and Automation*, Vol. 7, No. 6, December, 1991.
- [15] Smith, R. C., and Chessman, P., "On the Representation and Estimation of Spatial Uncertainty," *The International Journal of Robotics Research*, vol. 5, No. 4, 1986.
- [16] Su, S. F., and Lee, G. C. S., "Manipulation and Propagation of Uncertainty and Verification of Application of Actions in Assembly Tasks," *IEEE Transactions on Systems, Man, and Cybernetics*, Vol. 22, No. 6, Nov/Dec 1992.
- [17] Tarabanis, K., Tsai, T. Y., and Allen, P. K., "Automated Sensor Planning for Robotic Vision Tasks," *IEEE International Conference on Robotics and Automation*, Sacramento, CA, April, 1991.
- [18] Tarabanis, K., Tsai, R. Y., and Allen, P. K., "Analytic Characterization of the Feature Detectability Constraints of Resolution, Focus, and Field-of-View for Vision Sensor Planning," *CVGIP: Image Understanding*, Vol.59, No. 3, May, pp. 340-358, 1994.
- [19] Tarabanis, K., Tsai, R. Y., and Allen, P. K., "The MVP Sensor Planning System for Robotic Vision Tasks," *IEEE Transactions on Robotics and Automation*, Vol.11, No. 1, February, 1995.
- [20] Veitschegger, W. K., and Wu, C. H., "A Method for Calibrating and Compensating Robot Kinematic Errors," *IEEE International Conference on Robotics and Automation*, 1987.
- [21] Yang, C. C., Marefat, M. M., and Kashyap, R. L., "Active Visual Inspection Based on CAD Models," *Proceedings of IEEE International Conference on Robotics and Automation*, San Diego, CA, May 8 - 13, 1994.
- [22] Yang, C. C., Marefat, M. M., and Ciarallo, F. W., "Analysis of Errors in Dimensional Inspection Based on Active Vision," *Proceedings of SPIE International Symposium on Intelligent Robots and Computer Vision XIII: 3D Vision, Product Inspection, Active Vision*, Cambridge, MA, October 31- November 4, 1994.
- [23] Yang, C. C., and Marefat, M. M., "Spatial Quantization Errors in Active Vision Inspection," *Proceedings of IEEE International Conference on Systems, Man and Cybernetics*, San Antonio, TX, October 2-5, 1994.
- [24] Yang, C. C., and Marefat, M. M., "Flexible Active Computer Integrated Visual Inspection," *Proceedings of NSF Design and Manufacturing Conference*, Cambridge, MA, January 5-7, 1994.
- [25] Yang, C. C., and Marefat, M. M., "Object-Oriented Concepts and Mechanisms for Feature-Based Computer Integrated Inspection," *Advanced in Engineering Software*, vol. 20, 1995.
- [26] Yang, C. C., Marefat, M. M., and Ciarallo, F. W., "Analysis of Errors for Dimensional Inspection Using Active Vision Inspection," *IEEE Transactions on Robotics and Automation*, accepted for publication.
- [27] Yang, C. C., Marefat, M. M., Johnson, E., "Entity-based Aspect Graphs: Making the Viewer Centered Representation More Efficient", *Pattern Recognition Letters*, submitted.